Macromolecular Research, Vol. 23, No. 3, pp 284-290 (2015)
DOI 10.1007/s13233-015-3040-2

www.springer.com/13233
pISSN 1598-5032 eISSN 2092-7673

Fabrication of Natural Rubber/Epoxidized Natural Rubber/Nanosilica Nanocomposites and Their Physical Characteristics

Cuong Manh Vu*[,1], Huong Thi Vu[2], and Hyoung Jin Choi*[,3]

[1]*Chemical Department, Le Qui Don Technical University, 236 Hoang Quoc Viet, Ha Noi, Viet Nam*
[2]*AQP research and control pharmaceuticals Joint Stock Company (AQP Pharma J.S.C), 8 Chua Boc, Dong Da, Ha Noi, Viet Nam*
[3]*Department of Polymer Science and Engineering, Inha University, Incheon 402-751, Korea*

Received October 29, 2014; Revised December 30, 2014; Accepted December 30, 2014

Abstract: Epoxidized natural rubber (ENR) was initially prepared from an *in situ* performic acid epoxidation reaction with 46.09 mol% epoxide groups, and the curing characteristics of the ENR/natural rubber (NR) blend with different blend ratios of ENR were studied using a Monsanto moving die rheometer. The mechanical properties of the blends, such as the tensile strength, modulus at 300% elongation and elongation at break, were also examined. The tensile strength and 300% modulus decreased with increasing ENR content and the elongation at break increased steadily with increasing ENR content. In addition, the scorch time, cure time, maximum torque and torque difference decreased with increasing ENR content. Scanning electron microscopy (SEM) of the tensile fracture surfaces of the rubber blend samples revealed better compatibility between NR and ENR with lower ENR contents. Nanocomposites based on NR/ENR blends with two different ratios, 100/0 and 80/10, reinforced with 10 phr nanosilica were also prepared to examine the effects of ENR on the mechanical properties and morphology of the nanocomposites. SEM showed that ENR assists in the dispersion of nanosilica in the NR matrix, resulting in improved mechanical properties of the nanocomposite.

Keywords: epoxidized natural rubber, NR/silica nanocomposite, NR/ENR/silica nanocomposite, nanosilica.

Introduction

Although natural rubber (NR) latexes are one of the most important Vietnamese commercial products, they are mainly exported in their pristine form after being harvested because of less developed domestic industrial processing technology. Although NR has excellent mechanical characteristics, such as fatigue resistance and vibration reduction properties, its applications are limited by not only its low stability to heat, oxygen and light, but also its high solubility in most hydrophilic and hydrophobic solvents. Therefore, NR has been modified chemically to expand its applications and enhance its usage. Among these chemical modifications, the most successful one has been epoxidized NR (ENR), which is produced by attaching an oxygen atom to its carbon double bond. Consequently, ENR demonstrates oil resistance, gas-proof properties, and vibration reduction characteristics similar to some types of special rubber. For example, the oil resistance of ENR-50 containing 50 mol% epoxide groups is comparable to that of nitrile rubber with a medium nitril concentration and its gas-proof properties are similar to those of butyl rubber.[1] In addition, the chemical and physical properties of ENR, such as heat and swelling resistance, can change according to the epoxide content.[2] ENR also has higher polarity than virgin NR because of the presence of epoxide groups in its structure. In addition, it interacts with hydroxyl groups on the silica surfaces by hydrogen bonding mechanism due to its polar functional groups.[3] On the other hand, the mechanical properties of the silica-filled ENR without a coupling agent have been reported to be higher than those of silica-filled virgin NR,[4,5] as a result of the improved interactions between ENR and the silica surface *via* hydrogen bonding. Therefore, ENR as a rubber component in tire compounds has been reported to improve the silica dispersion, leading to improved processability, as well as better storage stability and tire performance.[3,6-8] ENR has also been used as a compatibilizer in silica-filled NR/acrylonitrile butadiene rubber (NBR) blends to enhance their mechanical properties.[9] In the case of silica-filled NBR vulcanates, the use of ENR as a compatibilizer improves the tensile strength, tear strength and abrasion loss,[10] while lowering the loss tangent,[11] because ENR can self-crosslink with NBR and link with silica at the vulcanization temperature because ENR acts as a coupling agent.[10-12] Furthermore, ENR has also been used as a compatibilizer in

*Corresponding Authors. E-mails: vumanhcuong309@gmail.com or hjchoi@inha.ac.kr

organoclay-filled NR composites, which improved the cure characteristics, tensile and dynamic mechanical properties.[13,14] Although ENR has been used to compatibilize silica and various rubber matrices, there have been few studies of use of ENR as a compatibilizer for silica-filled virgin NR.

Nanocomposites are defined as materials, in which the particle size of the dispersed phase is in the nanometer range, at least in one dimension.[14] Both silica and carbon black are reinforcing fillers that are used widely in various rubber industries. Because of their surface characteristics, both fillers tend to form agglomerates but the cause of this agglomeration is different, leading to a difference in dispersion ability. The filler-filler interactions of carbon black is generated mainly by the relatively weak van der Waals forces, which can be broken readily during mixing. In contrast, silica agglomeration is due mainly to hydrogen bonding in addition to van der Waals forces, and other physical interactions, leading to much stronger filler-filler interactions.[15] Furthermore, silica has both high polarity and a hydrophilic surface due to the presence of silanol groups on its surface. Consequently, silica is incompatible with non-polar rubber, such as NR, styrene-butadiene rubber (SBR) and butadiene rubber (BR), but is more compatible with polar rubbers, such as polychloroprene rubber (CR)[16] and NBR.[17] In addition, polar functional groups on the silica surface can form hydrogen bonds with other polar components in rubber compounds, such as accelerators. Therefore, common basic accelerators are adsorbed on the acidic surface of silica, which adversely affect the cure properties. Consequently, the successful use of silica nanoparticles for a rubber reinforcement requires silane coupling agents to enhance the silica-rubber interaction and silica dispersion, and prevent accelerator adsorption on the silica surface. Some polar rubbers bearing functional groups that can interact with the silica surface have been evaluated as alternatives to silane coupling agents with the aim of enhancing the interactions in silica-filled compounds.[18-21] The modified silica particles provide chemically active surfaces that can assist in vulcanization, providing coupling bonds between the silane and both the silica and rubber phases.[22-24] Those products show enhanced performance compared to their base materials. Furthermore, magnetic particle filled rubber systems have also drawn a huge attention as smart materials recently.[25]

This study examined the effects of the ENR content on the curing characteristics, tensile strength and morphology of NR/ENR blends with ENR contents varying from 0 to 100 parts per hundred (phr) as well as the effect of ENR as a compatibilizer on the morphology and mechanical properties of NR/silica nanocomposites. Vulcanizing accelerators were used with sulfur throughout the investigation.

Experimental

Materials. The rubbers used were NR (Standard Vietnamese Rubber-SVR 3L) and high ammonia NR latex containing approximately 0.65%-0.75% NH_3 to latex (w/w) to prevent spontaneous coagulation with 60 wt% of dry rubber purchased from PhuocHoa Rubber Joint Stock Co. ENRs with 46.3 mol% epoxide were prepared in-house, as explained in detail in the following section. The silica used as a filler for the NR/ENR blend was Ultrasil VN3 grade purchased from Evonik (SEA) Ltd. *N*-Cyclohexyl-2-benzothiazole sulfenamide (CBS), 2,2,4-trimetyl-1,2-dihydroquinolin (RD), and 2,2'-dibenzothizole disulfide (DM) purchased from Rongcheng Chemical Co. were used as the vulcanizing accelerators. ZnO, stearic acid, sulfur, and sodium dodecyl sulfate (SDS) were obtained from Sigma-Aldrich Chem. Co., Germany. Formic acid, hydrogen peroxide and ethanol from Shanghai Chemical Reagents, China were analytically pure reagents.

Sample Preparation. High ammonia (HA) NR latex with a 60 wt% dry rubber content (DRC) was diluted to a DRC of approximately 30% before being used to prepare the ENR *via* an *in situ* performic acid epoxidation reaction. The reaction between the C=C bond of the NR molecule and performic acid, arising from a reaction between formic acid and hydrogen peroxide (Figure 1), was carried out in a continuously stirred reactor at room temperature for 48 h, using the anionic surfactant, SDS, as a stabilizer. The ENR latex was neutralized with a 1% w/w $NaHCO_3$ solution and coagulated with ethanol. The coagulum was washed three times with distilled water and dried in an oven at 40 °C for 72 h. Figures 1 and 2 present the epoxidation reaction of NR latex and the general structure of ENR, respectively.

^{1}H nuclear magnetic resonance (NMR) (Bruker AVANCE, Germany) spectroscopy was used to analyze the molecular structure of NR and ENR. The spectra were obtained at 300 MHz using $CDCl_3$ as the solvent. The mol% of the epoxide groups was calculated using eq. (1).[26]

$$\text{mol\% of the epoxide group} = \frac{b}{a+b} \times 100 \quad (1)$$

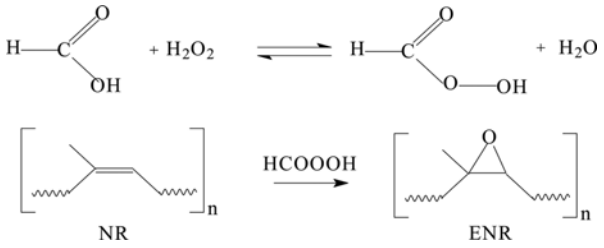

Figure 1. The epoxidation reaction of natural rubber.

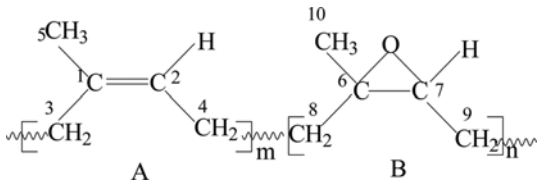

Figure 2. The general structure and the numbering of carbon atom in ENR employed in this work.

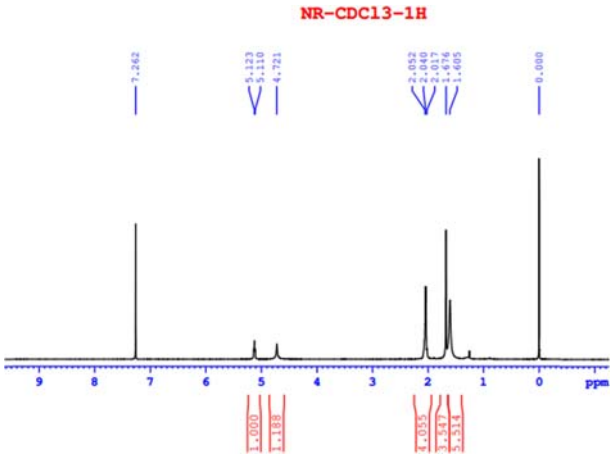

Figure 3. The ^{1}H NMR spectra of NR.

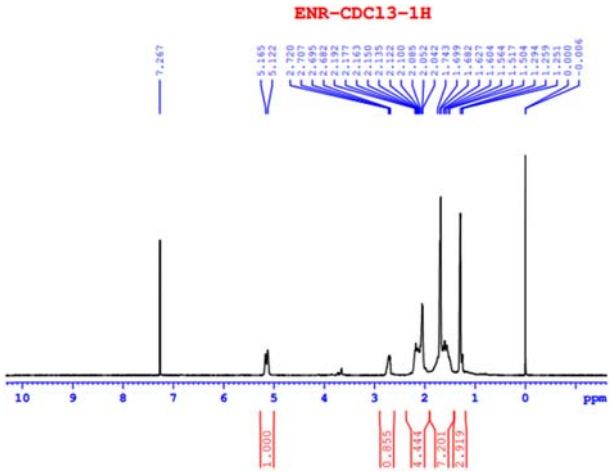

Figure 4. The ^{1}H NMR spectra of ENR.

where *a* is the integrated peak area of the olefinic proton of NR at 5.1 ppm and *b* is the integrated peak area of H attached to the oxirane rings of ENR at 2.7 ppm. Figures 3 and 4 show the ^{1}H NMR spectra of both NR and ENR, respectively.

The rubber compounds were prepared using the formulations as listed in Tables I and II. The ENR content was varied from 0 to 100 phr. NR, ENR and the ingredients, ZnO, stearic acid, paraffin, and silica, were added and mixed using an internal mixer (Brabender Plasticorder 350s, Germany) at a temperature of 50 ºC and rotor speed of 50 rpm. Mixing was further carried out using a two-roll mill after adding the vulcanizing accelerators of RD, CBS, and DM.

Cure Characterization and Curing. The cure characteristics of the rubber compounds were examined using a Monsanto moving die rheometer (model MDR2000P, USA) according to the ASTM 5289-12 method. Approximately 5 g of the rubber compound was placed between a pair of rotating discs at 150 ºC. The minimum torque (M_L), maximum (M_H), scorch time (t_2), and 90% of cure time (t_{90}) were then observed. Sheets, approximately 2 mm in thickness, were vulcanized in a Gotech (GT-7014-H molding test press, Taiwan) at 150 ºC and 40 kgf/cm^2 pressure for the respective cure times, t_{90}, derived from the MDR 2000P test.

The crosslinking density of the vulcanates was also measured from the stress-strain behavior according to the Mooney-Rilvin equation.[27,28]

Table II. Formulation for Different Amount of ENR with Silica

Ingredient	9	10
Natural Rubber	100	80
ENR	0	20
Zinc Oxide	5.0	5.0
Stearic Acid	3.0	3.0
Parafin	1.0	1.0
RD	2.5	2.5
CBS	1.5	1.5
DM	0.5	0.5
Sulfur	2,0	2,0
Silica	10	10

Table I. Formulation for Different Amount of ENR without Silica

Ingredient	1	2	3	4	5	6	7	8
Natural Rubber	100	90	80	70	60	40	20	0
ENR	0	10	20	30	40	60	80	100
Zinc Oxide	5.0	5.0	5.0	5.0	5.0	5.0	5.0	5.0
Stearic Acid	3.0	3.0	3.0	3.0	3.0	3.0	3.0	3.0
Parafin	1.0	1.0	1.0	1.0	1.0	1.0	1.0	1.0
RD	2.5	2.5	2.5	2.5	2.5	2.5	2.5	2.5
CBS	1.5	1.5	1.5	1.5	1.5	1.5	1.5	1.5
DM	0.5	0.5	0.5	0.5	0.5	0.5	0.5	0.5
Sulfur	2,0	2,0	2,0	2,0	2,0	2,0	2,0	2,0

$$\sigma = 2\left(\lambda - \frac{1}{\lambda^2}\right)\left(C_1 + \frac{C_2}{\lambda}\right) \quad (2)$$

where σ is the tensile stress, λ is the strain, and C_1 and C_2 are constants. A straight line could be drawn at the intermediate regions of the Mooney-Rivlin plot of $\sigma/(\lambda-\lambda^{-2})$ *vs*. $1/\lambda$, and $2C_1$ and $2C_2$ were calculated from the slope and intercept, respectively. The C_1 value can be used to assess the cross-linking density using eq. (3);

$$2C_1 = \rho kT \quad (3)$$

where ρ is the cross-linking density, k is the Boltzmann constant and T is the absolute temperature.

Mechanical Properties and Failure Behavior. The storage modulus (E'), loss modulus (E'') and mechanical loss factor ($\tan\delta = E''/E'$), as a function of temperature (T), were assessed by dynamic mechanical thermal analysis (DMTA) (Perkin Elmer DMA800, USA). DMTA was performed in tension mode at a 1 Hz frequency over a broad temperature range (T=-100 °C to +100 °C). The DMTA device was operated under a load control.

Tensile testing of five dumbbell shaped specimens cut from a mold sheet with a thickness of approximately 2 mm was conducted according to the ASTM D412-93 method. The tensile strength, elongation at break and tensile modulus (M300) were evaluated from the stress-strain determinations and the averages of five repeated tests for each compound were recorded.

Results and Discussion

Figures 3 and 4 show the ^{1}H NMR spectra of NR and ENR, respectively.

From Figure 4, the ^{1}H NMR chemical shift at δ1.30, δ2.72 and δ5.12-5.17 ppm was assigned to the methyl protons of B^{10}, the methine proton of B^7 and the methine proton of A^2, respectively. Note that B is an epoxy isoprene unit and A is an unepoxidized isoprene unit, as shown in Figure 2. The epoxy content of epoxidized rubber determined from eq. (1) was 46.09%. The appearance of peaks at δ1.30 ppm and δ2.72 ppm on the ^{1}H NMR of ENR, which were not observed in the ^{1}H NMR spectrum of NR, confirmed that the epoxidation reaction was complete.

Cure Characterization and Curing. Figure 5 and Table III present the rheograph and cure characteristics for the different NR/ENR blends, respectively. Regarding the data for the NR/ENR blends in Table III, both t_2 and t_{90} decreased with increasing ENR composition in the blends due to the activation of an adjacent double bond by the epoxide group in ENR. The scorch time and cure time for ENR were shorter than those of NR.[29]

The minimum torque, M_L, is related to the viscosity of the blends. The incorporation of ENR decreased slightly the minimum torque and the viscosity of the corresponding blends

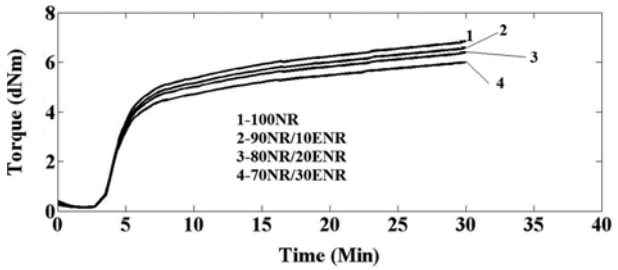

Figure 5. Reograph for different blend ratio of rubber compound between ENR and NR.

Table III. Cure Characteristic Data for Different Blend Ratio of Rubber Compound Between ENR and NR

NR/ENR	M_L	M_H	M_H-M_L	t_{90}	t_2
100/0	0.154	6.85	6.696	5.7	3.05
90/10	0.148	6.6	6.452	5.54	2.94
80/20	0.143	6.4	6.257	5.42	2.89
70/30	0.134	6	5.866	5.27	2.7

Table IV. The Tensile Properties of NR/Silica Nanocomoposite

Properties	Samples	
	NR100/Silica10	NR80/ENR20/Silica10
Tensile Strength (MPa)	15.7	26.2
300% Modulus (MPa)	1.32	1.19
Elongation at Break (%)	2630	2430

(Table III).

The maximum torque, M_H, which is the measure of the elastic stiffness of the vulcanized test specimen at the specified vulcanizing temperature, generally correlates with the durometer hardness and/or modulus.[30] Table IV shows that M_H decreases with increasing blend ratio of ENR in the blends, indicating that the incorporation of ENR decreases the stiffness of the blend. The torque difference (M_H-M_L), which indicates the extent of crosslinking,[31] showed a similar trend to the maximum torque. (M_H-M_L) is a measure of the dynamic shear modulus, which is related indirectly to the crosslinking density of the vulcanates, and decreases with increasing ENR incorporation. This might be because that the crosslinking density of the vulcanates decreases. The crosslinking density of the vulcanates was determined using the Mooney-Rilvin approach in eqs. (2) and (3).

Figure 6 shows the effect of the ENR contents on the crosslinking density of the NR/ENR blends, which decreases with increasing ENR incorporation. This observation is in line with that of the torque difference (M_H-M_L), which is an indirect measure of the crosslinking density. This is also related to the molecular structure of ENR. The crosslinking density of the ENR decreased significantly compared to NR because

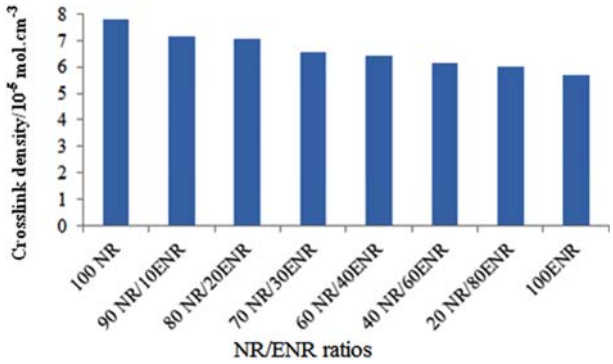

Figure 6. The effect of ENR contents on crosslink density of NR/ENR blends.

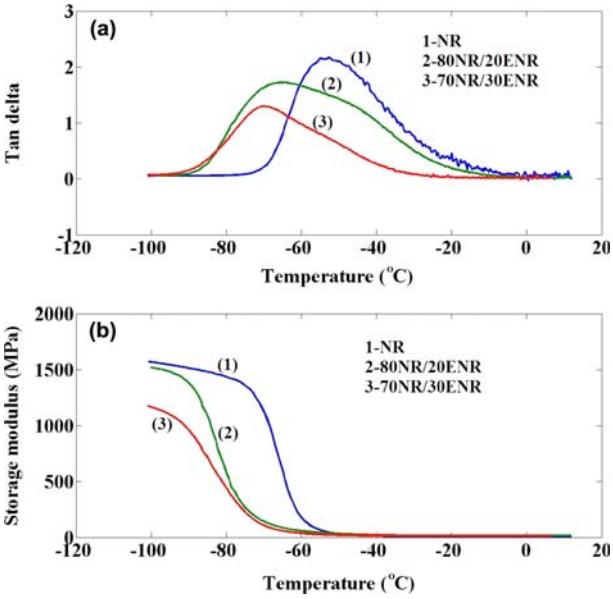

Figure 7. Effect of composition on the loss tangent (a) and the storage modulus E' (b) of the NR component of the NR/ENR blends.

ENR contains an oxirane ring, meaning that the number of C=C bonds decreases.

For the NR/ENR blends, despite the increase in ENR content, the crosslinking density of the blends decreased because of a decrease in the total number of C=C bonds.

Mechanical Property. Figure 7 shows the dynamic storage modulus (E') and mechanical loss factor (tanδ) *vs*. temperature (T) traces for the NR/ENR blends.

The DMTA is one of the most widely used techniques for determining the miscibility between the components in the blends, and it is accepted that a single glass transition would result in the complete mixing of components at the molecular level. Figure 7 shows the effect of the composition on the loss tangent of the NR component for the NR/ENR blends. T_g was taken as the tanδ maximum temperature. Compared to NR, the T_g of the NR component in the NR/ENR blends containing 20-80 wt% ENR shifted to lower temperatures by 10-15 °C (Figure 7). The T_g of the NR/ENR blends with

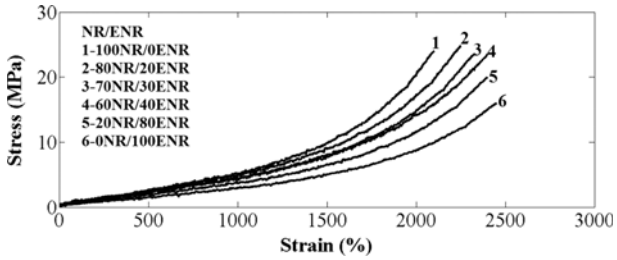

Figure 8. Stress-strain of NR/ENR blends.

ratios of 100/0, 80/20, and 70/30 were -50.18, -64.15, and -70.28 °C, respectively. The T_g of the NR/ENR blends decreased with increasing ENR contents due to the decrease in crosslinking density.

Tensile Property and Morphology. Figure 8 presents the typical stress-strain curves of the NR/ENR blends, showing that all stress-strain curves of the NR/ENR blends are characterized by the rapidly rising slope when the strain reaches more than 1500%, due to the deformation-induced crystallization.[32,33] On the other hand, the degree of the increase in the curve slope decreased with increasing levels of ENR.

Figure 9 shows the effects of ENR on the tensile strength, elongation at break and M300 (moduli at 300% elongations) of the NR/ENR blends, showing that the tensile strengths were relatively constant at NR/ENR ratios ranging from 100/0 to 60/40. In contrast, when the NR/ENR ratios ranged from 60/40 to 0/100, the tensile strength decreases significantly to that of ENR. The results from Figure 9(a), (b), and (c) also show that the tensile strength and 300% modulus of the cured ENR sample (NR/ENR=0/100) were 18.2 and 0.95 MPa, respectively, which are significantly lower than the 24 and 1.3 MPa observed for the NR sample (NR/ENR=100/0). On the other hand, the elongation at break of the ENR sample was 2450%, which is significantly higher than that of the NR sample (2100%).

The change in tensile strength, elongation to break and 300% modulus at different ENR contents is related to the crosslinking density of the blends. The crosslinking density of the NR/ENR blends decreased with increasing ENR content, leading to a decrease in the 300% modulus and an increase in the elongation at break due to increased slipped level between the different molecular chains. Both ENR and NR are likely to crystallize when stretching, but the degree of crystallization of ENR when stretching is smaller than that with NR. As a result, ENR has a lower tensile strength than NR. In the case of the NR/ENR blends, when ENR was the dispersed phase, the tensile strength of the NR/ENR blends did not decrease significantly when the ENR contents were 10, 20, 30, and 40 phr. In contrast, the tensile strength of the blends with 60 and 80 phr ENR decreased rapidly.

Figure 10 presents SEM images of the tensile fracture surfaces of NR/ENR blends at different ratios.

Considering the tensile mechanical data in Figure 9 and the

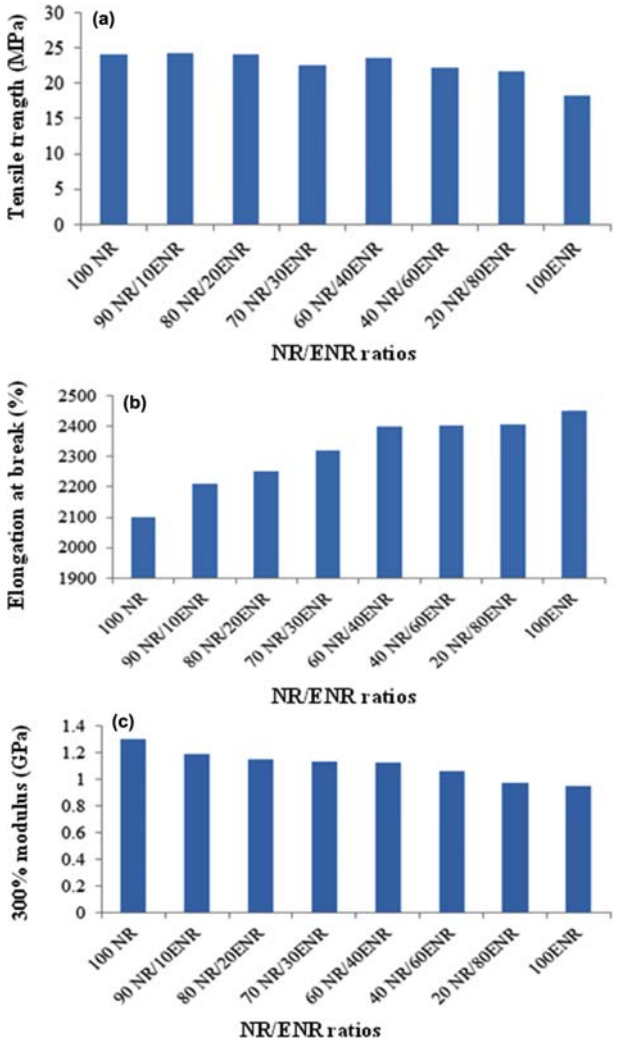

Figure 9. Effect of composition on the tensile strength (a), 300% modulus (b) and elongation at break (c) for the NR/ENR blends.

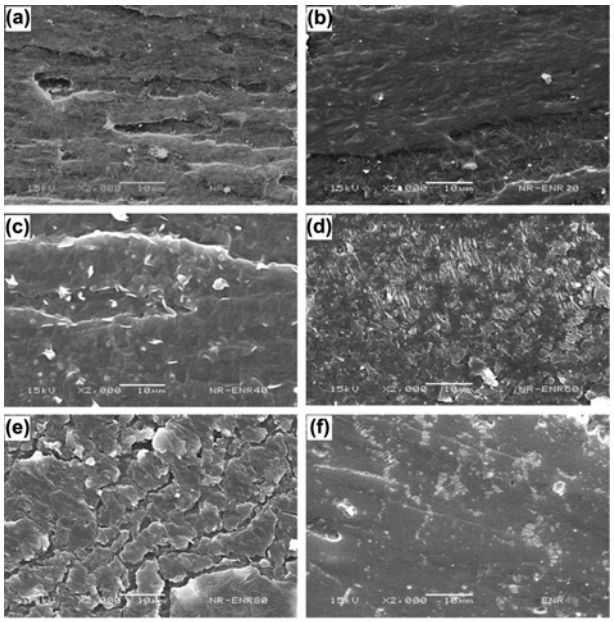

Figure 10. SEM micrographs showing tensile fracture surface of NR/ENR blends with different ratio ((a) 100NR/0ENR, (b) 80NR/20ENR, (c) 60NR/40ENR, (d) 40NR/60ENR, (e) 20NR/80ENR, (f) 0NR/100ENR).

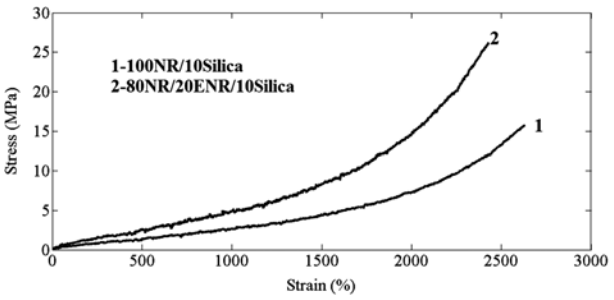

Figure 11. Stress-strain of NR/silica nanocomposites.

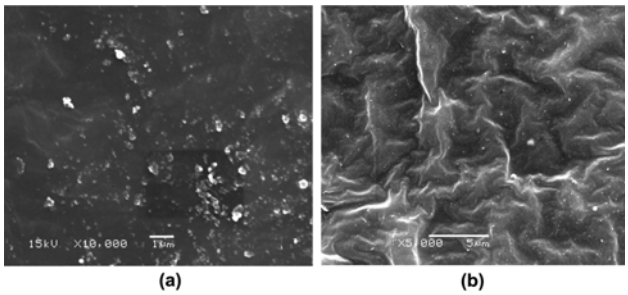

Figure 12. SEM micrographs showing tensile fracture surface of NR100/silica10 (a) and NR80/ENR20/silica10 (b) nanocomposites.

fracture surfaces in Figure 10, the fractured surface of NR (Figure 10(a)) was rougher; hence, more energy was required. The fracture surface of the NR/ENR blends become smooth when the ENR content was increased (Figure 10(b), (c)). The phase separation can be observed in Figure 10(d) and (e) for NR/ENR ratios of 40/60 and 20/80, respectively, in which ENR is the main phase and NR is the dispersed phase. Compared to NR, ENR showed a smoother fracture surface (Figure 10(f)) and fewer horizontal tearing lines. This is consistent with the results showing that the tensile strength of NR is higher than that of ENR.

The 80NR/20ENR ratio was chosen to study the effect of ENR on the mechanical and morphology properties of the nanocomposite from both NR and nanosilica.

Figure 11 and Table IV show that the tensile strength of the uncompatibilized NR/silica nanocomposite decreased moderately when filled with 10 phr silica, whereas the tensile strength of the nanocomposites increased significantly after adding the ENR compatibilizer compared to the NR sample. This improvement was attributed to the filler (*i.e.* silica) dispersion and filler/matrix adhesion.

The tensile fracture surfaces were observed by SEM to better understand the effects of ENR on the mechanical properties of the NR/silica nanocomposites.

Figure 12 shows that the silica still existed in a state of aggregation in the tensile fracture surface of the NR100/silica10 sample. In contrast, the surface of NR80/ENR20/silica 10 was rougher with a better dispersion of silica. This suggests that ENR helps improve the filler-rubber interaction, *i.e*., silica dispersion, and increases the tensile strength.

Conclusions

By adding ENR, which was prepared by an *in situ* performic acid epoxidation reaction in the NR, both the scorch and cure times decreased due to the activation effects of the epoxy functional groups on crosslinking. The crosslinking density, tensile strength and 300% modulus of the NR/ENR blends decreased with increasing ENR content, whereas ENR helped improved the elongation at break. In addition, the use of ENR as a compatibilizer in silica-filled natural rubber nanocomposites resulted in improved silica dispersion and tensile strength.

References

(1) I. R. Gelling, *Rubber Chem. Technol.*, **58**, 86 (1985).
(2) I. R. Gelling and M. Porter, in *Natural Rubber Science and Technology*, A. D. Robert, Ed., Oxford University Press, Oxford, 1988, Chap. 10.
(3) H. Y. Xu, J. W. Liu, L. Fang, and C. F. Wu, *J. Macromol. Sci. B: Phys*., **46**, 693 (2007).
(4) F. Cataldo, *Macromol. Mater. Eng*., **287**, 348 (2002).
(5) Y. Y. Luo, Y. Q. Wang, J. P. Zhong, C. Z. He, Y. Z. Li, and Z. Peng, *J. Inorg. Organomet. Polym*., **21**, 777 (2011).
(6) S. Varughese and D. K. Tripathy, *J. Appl. Polym. Sci*., **44**, 1847 (1992).
(7) S. Schaal, A. Y. Coran, and S. K. Mowdood, US Patent 6482884 B1 (2002).
(8) C. J. Lin and W. L. Hergenrother, US Patent 6845797 B2 (2005).
(9) C. Kantala, E. Wimolmala, C. Sirisinha, and N. Sombatsompop, *Polym. Adv. Technol*., **20**, 448 (2009).
(10) K. M. George, J. K. Varkey, K. T. Thomas, and N. M. Mathew, *J. Appl. Polym. Sci*., **85**, 292 (2002).
(11) S. Karnda, S. Kannika, K. D. Wilma, and W. M. Jacques, *Eur. Polym. J*., **51**, 69 (2014).
(12) W. D. N. Ayutthaya and S. Poompradub, *Macromol. Res*., **22**, 686 (2014).
(13) P. L. Teh, Z. A. MohdIshak, A. S. Hashim, J. Karger-Kocsis, and U. S. Ishiaku, *J. Appl. Polym. Sci*., **94**, 2438 (2004).
(14) P. L. Teh, Z. A. MohdIshak, A. S. Hashim, J. Karger-Kocsis, and U. S. Ishiaku, *Eur. Polym. J*., **40**, 2513 (2004).
(15) O. Seyvet and P. Nevard, *J. Appl. Polym. Sci*., **78**, 1130 (2000).
(16) A. Das, S. C. Debnath, D. De, and D. K. Basu, *J. Appl. Polym. Sci*., **93**, 196 (2004).
(17) S. S. Choi, *J. Appl. Polym. Sci*., **79**, 1127 (2001).
(18) H. Ismail and H. H. Chia, *Eur. Polym. J*., **34**, 1857 (1998).
(19) H. Ismail, A. Rusli, and A. A. Rashid, *Polym. Test*., **24**, 856 (2005).
(20) A. K. Manna, A. K. Bhattacharyya, P. P. De, D. K. Tripathy, S. K. De, and D. G. Peiffer, *Polymer*, **39**, 7113 (1998).
(21) N. Suzuki, M. Ito, and S. Ono, *J. Appl. Polym. Sci*., **95**, 74 (2005).
(22) I. Surya, H. Ismail, and A. R. Azura, *Polym. Test*., **40**, 24 (2014).
(23) P. Sae-oui, C. Sirisinha, U. Thepsuwan, and K. Hatthapanit, *Eur. Polym. J*., **42**, 479 (2006).
(24) S. J. Park, K. S. Kim, and B. J. Kim, *J. Adhes. Sci. Technol*., **26**, 861 (2012).
(25) J. H. Yoon, I. H. Yang, U. C. Jeong, K. H. Chung, J. Y. Lee, and J. E. Oh, *Polym. Eng. Sci.*, **53**, 992 (2013).
(26) D. R. Burfield, K. Lim, K. Law, and S. Ng, *Polymer*, **25**, 995 (1984).
(27) A. A. M. Ward, B. Stoll, W. von Soden, S. Herminghaus, and A. A. Mansour, *Macromol. Mater. Eng*., **288**, 971 (2003).
(28) L. Mullins, *J. Polym. Sci*., **19**, 225 (1956).
(29) B. T. Poh, H. Ismail, E. H. Quah, and P. L. Chin, *J. Appl. Polym. Sci.*, **81**, 47 (2001).
(30) H. Ismail and B. T. Poh, *Eur. Polym. J*., **36**, 2403 (2000).
(31) M. T. Ramesan, G. Mathew, B. Kuriakose, and R. Alex, *Eur. Polym. J*., **37**, 719 (2001).
(32) S. Toki and B. S. Hsiao, *Macromolecules*, **36**, 5915 (2003).
(33) J. M Chenal, L. Chazeau, L. Guy, Y. Bomal, and C. Gauthier, *Polymer*, **48**, 1042 (2007).